ACS Medicinal Chemistry Letters

Letter

pubs.acs.org/acsmedchemlett

Evaluation and Structural Basis for the Inhibition of Tankyrases by PARP Inhibitors

Teemu Haikarainen,[†,∥] Mohit Narwal,[†,‡,∥] Päivi Joensuu,[§] and Lari Lehtiö*[,†]

[†]Biocenter Oulu, Department of Biochemistry, University of Oulu, Oulu, Finland

[‡]Pharmaceutical Sciences, Department of Biosciences, Abo Akademi University, Turku, Finland

[§]Department of Chemistry, University of Oulu, Oulu, Finland

Supporting Information

ABSTRACT: Tankyrases, an enzyme subfamily of human poly(ADP-ribosyl)polymerases, are potential drug targets especially against cancer. We have evaluated inhibition of tankyrases by known PARP inhibitors and report five cocrystal structures of the most potent compounds in complex with human tankyrase 2. The inhibitors include the small general PARP inhibitors Phenanthridinone, PJ-34, and TIQ-A as well as the more advanced inhibitors EB-47 and rucaparib. The compounds anchor to the nicotinamide subsite of tankyrase 2. Crystal structures reveal flexibility of the ligand binding site with implications for drug development against tankyrases and other ADP-ribosyltransferases. EB-47 mimics the substrate NAD^+ and extends from the nicotinamide to the adenosine subsite. The clinical ARTD1 inhibitor candidate rucaparib was the most potent tankyrase inhibitor identified (24 and 14 nM for tankyrases), which indicates that inhibition of tankyrases would affect the cellular responses of this compound.

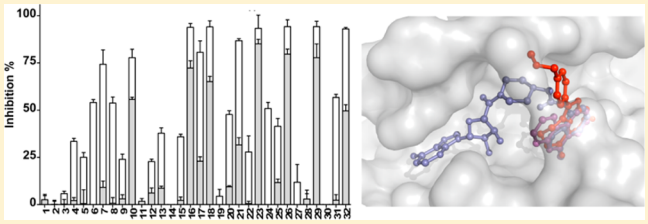

KEYWORDS: *Tankyrase, ADP-ribosyltransferase, poly(ADP-ribose) polymerase, PARP, inhibitor*

Poly(ADP-ribose)polymerase 1 (PARP-1/ARTD1) has been a promising drug target especially since the discovery of its role in DNA repair and the synthetic lethality of PARP inhibitors in cancers deficient in DNA repair.[1] Over the years inhibitors for the enzyme with improved potency have been identified and several are currently in clinical trials.[2] The enzyme family, which contains 17 members in humans, catalyzes ADP-ribosylation, a covalent post-translational protein modification. Many of these enzymes play critical roles in various cellular pathways, although in some cases their exact roles remain to be elucidated. Tankyrases are members of the human PARP superfamily also called Diphtheria toxin-like ADP-ribosyltransferases (ARTDs). They contain a catalytic ART domain in the C-terminus with an adjacent sterile alpha motif responsible for the oligomerization of the enzyme.[3] A major part of tankyrases is formed by 24 ankyrin repeats that recognize the target protein to be modified. Human tankyrase 1 (ARTD5/TNKS1/PARP-5a) and tankyrase 2 (ARTD6/TNKS2/PARP-5b) are homologous with 82% sequence identity, but ARTD5 contains an additional N-terminal histidine, proline, and serine rich region with an unknown function. Tankyrases are involved in various cellular pathways, such as telomere homeostasis, mitosis, GLUT4 vesicle transport, and Wnt signaling, which make them possible targets for therapy.[4,5] Especially their role in Wnt signaling suggests they could be used to treat cancers that have excessive activation of the Wnt pathway.[6] The small molecules that inhibit ARTDs and tankyrases bind to the catalytic ART domain, which is highly conserved between ARTD5 and ARTD6 with 89% sequence identity.

To evaluate tankyrases as potential drug targets we screened a small library of PARP inhibitor like compounds against tankyrases using an activity-based screening method.[7] This, combined with X-ray crystallography, would potentially help to characterize the structural features of potent tankyrase inhibitors and thus provide new scaffolds that could be optimized to specifically target tankyrases.

PARP inhibitors and close analogues were initially screened against ARTD5 at 10 μM concentration. The compounds were selected from the literature and purchased from commercial vendors. Of the 32 compounds tested, 14 showed over 50% inhibition of the enzyme (Figure 1 and Table S1, Supporting Information). However, compound **4** (Veliparib), which has a single digit nanomolar affinity for ARTD1 and ARTD2, showed only 33% inhibition at this concentration. In order to clearly identify the most potent ARTD5 inhibitors, the screen was repeated at 500 nM concentration. Nine compounds still showed more than 20% inhibition, and these were selected for further characterization and structural analysis. All the compounds have a motif similar to nicotinamide and therefore would be expected to compete with the substrate (Figure 1). Five of the compounds have already been described as

Received: July 27, 2013
Accepted: November 20, 2013
Published: November 20, 2013

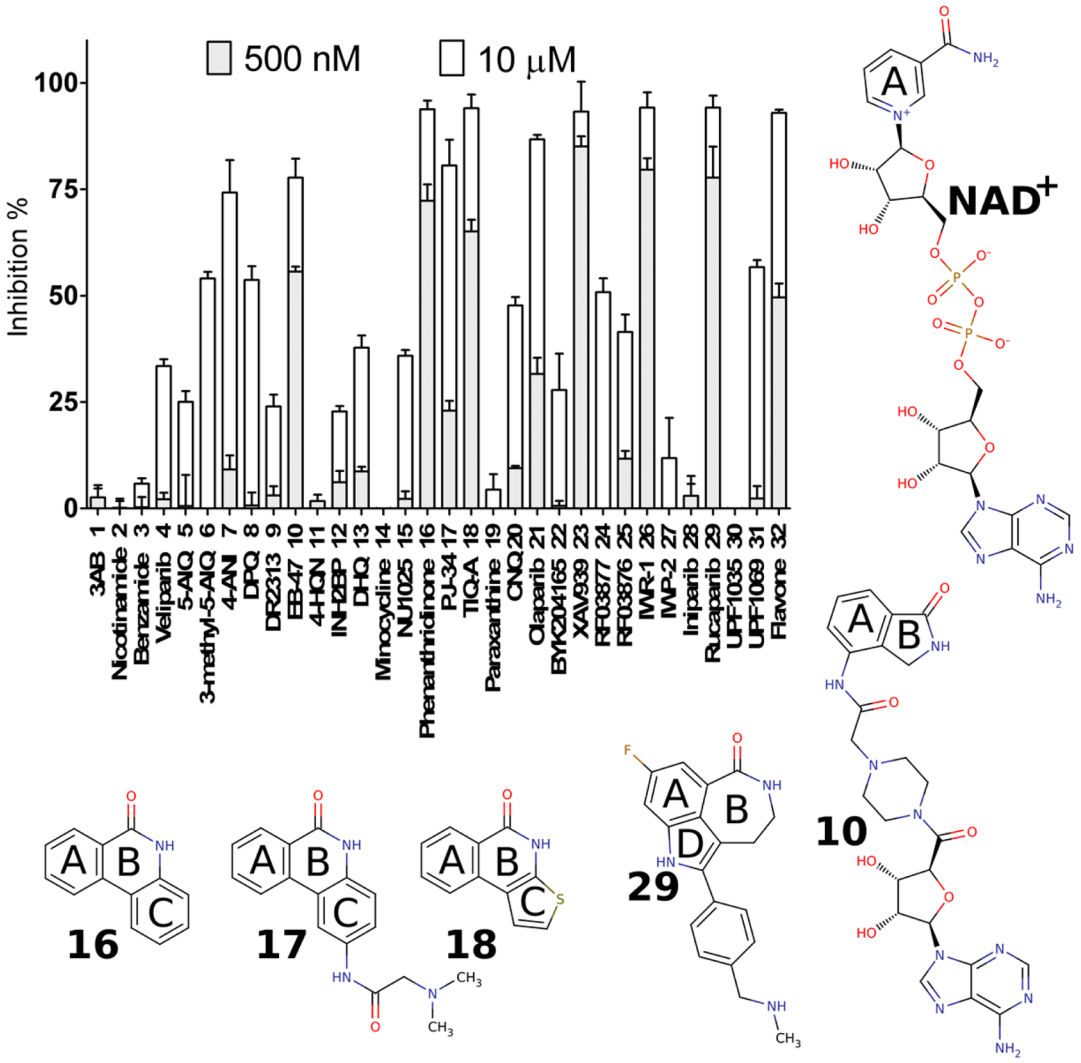

Figure 1. Screening of PARP inhibitor compounds and the structures of the potent hit compounds. At 10 μM many of the compounds inhibited ARTD5, whereas a test at 500 nM identified 9 compounds that showed over 20% inhibition. Data shown are mean ± SD.

tankyrase inhibitors and have also been characterized using protein crystallography: **17** (PJ-34; ARTD5 IC50 570 nM),[8,9] **21** (Olaparib; ARTD5 IC50 1500 nM),[10,11] **23** (XAV939; ARTD5 IC50 11 nM),[12,13] **26** (IWR-1; ARTD5 IC50 130 nM),[10] and **32** (flavone; ARTD5 330 nM).[7,14] In this study, we characterized the binding mode of the four additional compounds using X-ray crystallography: **10** (EB-47),[15] **16** (phenanthridinone),[16] **18** (TIQ-A),[17] and **29** (rucaparib).[18] As **17** (PJ-34) has also been reported to bind to a distinct adenosine binding groove of the catalytic domain we included this compound in further studies.[8,19]

From the five compounds two are phenanthridinones (**16** and **17**) and one, **18**, resembles phenanthridinones in shape as it also consists of 3 fused aromatic rings (Figure 1). Compound **29** also contains a three ring system, but the seven-membered ring is not aromatic and the three rings are organized differently with respect to the nicotinamide-like moiety. Compound **29** also has a (methylaminomethyl)phenyl substituent. Compound **10** was designed to mimic NAD^+, and it contains an adenosine connected to the nicotinamide mimic with a long linker replacing the ribose-diphosphate part of NAD^+ (Figure 1).[15]

The measured IC_{50} values agree well with the ranking of the compounds in the single data point screening (Table 1 and Figure 1). The small tricyclic compounds **16** and **18** show potencies of 110 and 200 nM, respectively, whereas the derivative of **16** with a substitution, **17**, shows lower potency (1300 nM) consistent with the values reported in the literature (570−1000 nM).[8,9] Compound **10** is a large polar inhibitor (calculated logP −2.55) that shows moderate potency against ARTD5 (410 nM). The most potent inhibitor, however, is the

Table 1. Potencies of the Characterized Compounds[a]

compd	ARTD5 IC_{50} (log IC_{50} ± SEM)	ARTD6 IC_{50} (log IC_{50} ± SEM)	ARTD1 (from literature)
EB-47 (**10**)	410 nM (6.39 ± 0.10)	45 nM (7.35 ± 0.04)	45 nM (IC_{50})[15]
phenanthridinone (**16**)	110 nM (6.95 ± 0.15)	14 nM (7.86 ± 0.05)	300 nM (IC_{50})[16]
PJ-34 (**17**)	1300 nM (5.87 ± 0.12)	219 nM (6.66 ± 0.02)	20 nM (EC_{50})[19]
TIQ-A (**18**)	200 nM (6.70 ± 0.09)	24 nM (7.62 ± 0.01)	450 nM (IC_{50})[17]
rucaparib (**29**)	25 nM (7.60 ± 0.14)	14 nM (7.85 ± 0.07)	1.4 nM (K_i)[18]

[a]The measurements were carried out three (**10**, **16**, **18**, and **29**) or four times (**17**), and dose response curves were fitted individually.

dx.doi.org/10.1021/ml400292s | ACS Med. Chem. Lett. 2014, 5, 18−22

clinical candidate targeted against ARTD1, **29**, which shows an IC_{50} value of 25 nM making this one of the best scaffolds among tankyrase inhibitors. Notably, these compounds are even better ARTD6 inhibitors (Table 1).

Both **16** and **18** bind in a similar fashion to the nicotinamide subsite of the catalytic domain of ARTD6 (Figure 2a,b). Like

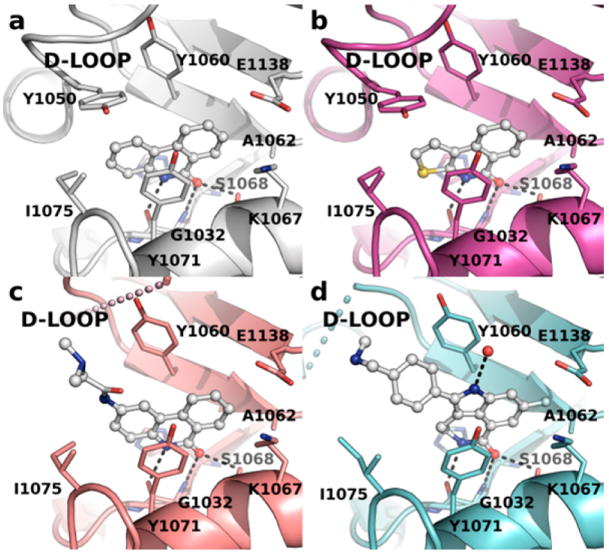

Figure 2. Crystal structures of (a) phenanthridinone (**16**), (b) TIQ-A (**18**), (c) PJ-34 (**17**), and (d) rucaparib (**29**) bound to the ARTD6 catalytic fragment. The compounds are shown as ball-and-stick models and the hydrogen bonds with the protein are shown as dashed lines. The disordered D-loop in panels c and d is shown as a thick dashed line.

many ARTD inhibitors, they form a $\pi-\pi$ stacking interaction with Tyr1071 and make the typical hydrogen bonds at the end of the nicotinamide pocket with Ser1068 and Gly1032. The compounds also form hydrophobic interactions with Tyr1060 and Lys1067. In addition, the third aromatic C-rings of these compounds form hydrophobic interactions with the Tyr1050 and Ile1075 that close the binding groove. The structures of **16** and **18** are very similar, and there are no significant differences between the crystal structures of their protein complexes. The small differences in the measured IC_{50} values may be caused by more efficient hydrophobic interactions of the six membered C-ring of phenanthridinone (Table 1 and Figure 2). The binding pocket in tankyrases is more hydrophobic,[9] and in particular, Tyr1050 and Ile1075 are not conserved in ARTD1.

The binding site of **17** in the nicotinamide pocket is very similar to that of **16** and **18**, and it forms stacking interactions and hydrogen bonds with ARTD6 similar to those of the other compounds. Compound **17** is based on a phenanthridinone scaffold and contains a long dimethylamino acetamide tail attached to the C-ring (Figure 2). This tail causes opening of the D-loop (Figure 2c). The D-loop is not resolved in the observed electron density map, and therefore, it is apparently flexible and does not form stable interactions with compound **17**. The tail of **17** is also flexible and has diffuse electron density. As Tyr1050 of the D-loop is moved out of the binding pocket, Tyr1060 rotates 15 degrees toward compound **17** with respect to the complex structure of **16**. Compound **17** does not bind as deeply into the pocket as **16** and **18** and the hydrogen bond between the compound **17** amide and the carbonyl of Gly1032 is longer (2.9 Å vs 2.7 Å). Previously a cocrystal structure of ARTD5 with **17** was reported, with two molecules of **17** bound to the catalytic domain: one to the nicotinamide site and one to the adenosine binding subsite.[8] Despite the opening of the D-loop upon soaking of the crystals, we observed binding of only one molecule of **17** to the catalytic domain of ARTD6.

Compound **29** is a large (323 Da) and optimized ARTD1 inhibitor containing a nicotinamide-like motif fused to a seven-membered B-ring (Figure 1). The compound binds to the nicotinamide pocket and forms the stacking interaction with Tyr1071 and hydrogen bonds with Ser1068 and Gly1032 (Figure 2d). Like **17**, **29** does not bind as deeply into the pocket as **16** and **18** (distance to Gly1032 = 2.9 Å). The fluorine atom interacts with the hydrophobic part of the catalytic Glu1138 and with Ala1062. The seven-membered nonplanar B-ring does not make any distinct interactions within the active site. The amide of the D-ring is hydrogen bonded to a water molecule (Figure 2d), which is connected to a water network. The (methylaminomethyl)phenyl substituent extends from the nicotinamide site in the same direction as the tail of **17**, and this causes large changes in the active site. The D-loop opens up and becomes completely disordered in the crystal structure. The bulky phenyl group also causes a change in the conformation of Ile1075 and rotation of Tyr1060 (15 degrees) and of Tyr1071 (30 degrees) with respect to the other complex structures (Figure 2). This makes the Tyr1071 completely parallel with the aromatic D-ring of the compound.

The binding of **17** and **29** cause disordering of the D-loop (Figure 2c,d) lowering the potency of **17** in comparison to **16** and **18**. In the case of **29**, the additional interactions made by the tricyclic core and the efficient stacking of the compound with aromatic residues at the active site overcomes this, and the compound shows remarkably good potency as a tankyrase inhibitor. The D-loop is very dynamic and often adopts new conformations in order to accommodate the inhibitors.[10] As compound **29** is a potent tankyrase inhibitor, it is possible that some of the observed clinical effects could be due to tankyrase inhibition especially in cases where β-catenin expression is enhanced.[20,21]

Compound **10** was designed to mimic NAD^+ and to bind to the substrate NAD^+ site of ARTD1.[15] The crystal structure of **10** in complex with ARTD6 shows that the compound binds to the NAD^+ binding groove of ARTD6 and spans all the way from the nicotinamide binding subsite to the adenosine subsite of this cleft (Figure 3a). At the nicotinamide site the isoindolinone moiety makes the typical hydrogen bonds to Gly1032 and to Ser1068 (Figure 3a). The compound induces opening of the D-loop, but in contrast to the complex structures with **17** and **29**, the D-loop is visible in the crystal structures. Tyr1050, which plays a critical role in the binding of **16** and **18**, moves out of the pocket and faces solvent. The carbonyl of the linker region makes a water-mediated interaction with the backbone of Tyr1060, but the rest of the interactions made by the linker are hydrophobic. Ribose hydroxyls are coordinated by residues that are conserved in most of the ARTD enzymes: His1031 and Ser1033 (Figure 3a). In addition, ribose interacts with Gly1032 via a water molecule. The adenosine group of **10** binds between an α-helix and the His1048 of the D-loop. It also forms hydrogen bonds with the backbone atoms of Gly1043 and Asp1045 (Figure 3a).

There are no substrate NAD^+ bound structures available for any of the human ARTD enzymes. As **10** somewhat resembles NAD^+ (Figure 2), the crystal structure makes it possible to

dx.doi.org/10.1021/ml400292s | ACS Med. Chem. Lett. 2014, 5, 18−22

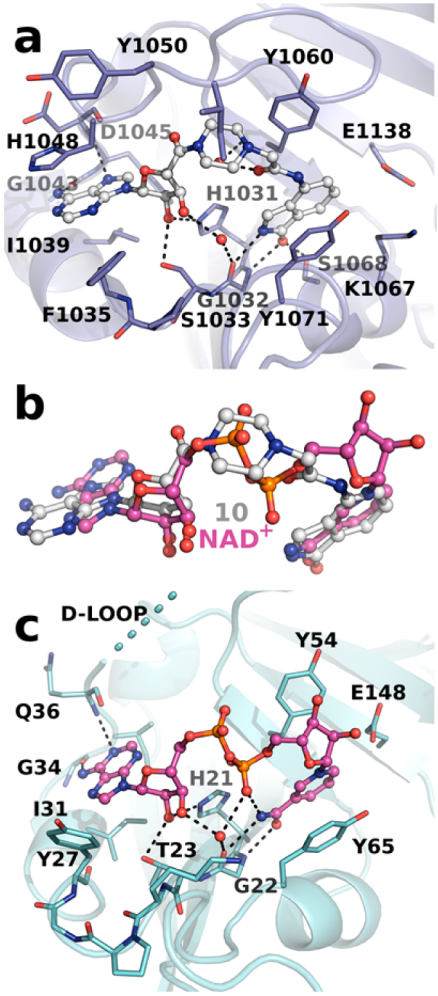

Figure 3. Binding of the dual site inhibitor EB-47 (**10**) and comparison of the structure with the substrate NAD^+ binding mode to Diphtheria toxin. (a) Binding mode of EB-47 to ARTD6. (b) Comparison of superposed EB-47 with NAD^+ bound to Diphtheria toxin (PDB code 1TOX). Superposition was done with selected atoms in order to overlap adenosine and nicotinamide moieties. (c) NAD^+ complex conformation observed in Diphtheria toxin (PDB code 1TOX). The disordered D-loop is shown as a dashed line.

analyze the potential substrate binding conformation. NAD^+ bound to Diphtheria toxin crystals (PDB code 1TOX) can be superposed with **10** bound to ARTD6 (Figure 3b). Overall the conformation is similar but there are major differences especially at the adenosine moiety, which has been rotated by 180 degrees in **10**. This may therefore indicate that the binding mode of NAD^+ in human ARTDs or in tankyrases could be distinct from the toxin or that the rotation could be just a property of the inhibitor.

The binding of **10** to the nicotinamide subsite closely resembles the binding mode of NAD^+ observed in the crystal structure, and the residues surrounding this site are mostly conserved, such as a glycine that forms two of the hydrogen bonds to the amide and the tyrosines lining the sides of the pocket (Figure 3). The linker replacing a ribose and phosphate parts of the substrate is 2 atoms shorter than in NAD^+, but despite this, the region overlaps well with the substrate. Neither NAD^+ nor **10** make specific interactions with the D-loop, and this region is not even visible in the toxin structure (Figure 3c).[22]

The adenosine ribose of NAD^+ is coordinated by residues conserved in tankyrases: His21, Thr23, and a water molecule (Figure 3c). The adenosine forms two hydrogen bonds to the backbone atoms at the delta of the binding groove. The histidine that forms a $\pi-\pi$ stacking interaction with **10** in ARTD6 is not present in the diphtheria toxin. Also other recently discovered inhibitors form this stacking interaction.[10,23,24] As the subsite is conserved in tankyrases, this could indicate a unique binding mode of the substrate in tankyrases although both orientations of the adenosine are possible.

We have described a structural basis of the inhibition of tankyrases by selected potent inhibitors. This could be utilized in further development of inhibitor scaffolds. The complex structure of ARTD6 with **10** gives indications of the binding mode of the substrate and leaves the role of the D-loop in substrate binding as a question to be studied in the future. This analysis also relates to ARTD inhibitor development as the clinical candidates against ARTD1 included in the analysis showed different responses in the assay. Compound **4** was not a potent inhibitor of tankyrase (IC_{50} > 10 μM), **28** (Iniparib) did not show any inhibition, **21** showed some inhibition in agreement with the reported IC_{50} value of 1500 nM, and **29** was identified as a very potent tankyrase inhibitor. It is evident that the PARP inhibitor selectivity profile should be taken into account when planning experiments. The results also indicate that the different specificity of the tested clinical candidates could affect the efficacy and cause varying side effects in clinical studies.

■ ASSOCIATED CONTENT

Supporting Information

Supplementary Table 1 contains details of the compound library. Supplementary Table 2 contains statistics of the crystallographic data and refinement of the structures. This material is available free of charge via the Internet at http://pubs.acs.org.

Accession Codes

Coordinates and structure factors are deposited to the Protein Data Bank with codes 4BJ9, 4AVU, 4BJB, 4AVW, and 4BJC.

■ AUTHOR INFORMATION

Corresponding Author

*(L.L.) Phone: +358 2 9448 1169. E-mail: lari.lehtio@oulu.fi.

Author Contributions

‖These authors (T.H. and M.N.) contributed equally to this work.

Funding

The work was funded by Biocenter Oulu. T.H. was supported by funding from the Academy of Finland (grant No. 266922). M.N. is a member of the National Doctoral Programme of Informational and Structural Biology. This work was carried out with the support of the Diamond Light Source (Didcot, U.K.) and the European Synchrotron Radiation Facility (ESRF, Grenoble, France). The research leading to these results has received funding from the European Community's Seventh Framework Programme (FP7/2007−2013) under BioStruct-X (grant agreement No. 283570).

Notes

The authors declare no competing financial interest.

■ ACKNOWLEDGMENTS

We are grateful to local contacts at ESRF and at Diamond for providing assistance in using beamlines ID14-1, ID23-2, and I04-1. We also thank Erik Rannaste and Sari Ek for the analysis of the compounds.

■ ABBREVIATIONS

ART, ADP-ribosyltransferase; PARP, poly(ADP-ribose) polymerase; TNKS, tankyrase

■ REFERENCES

(1) Bryant, H. E.; Schultz, N.; Thomas, H. D.; Parker, K. M.; Flower, D.; Lopez, E.; Kyle, S.; Meuth, M.; Curtin, N. J.; Helleday, T. Specific Killing of BRCA2-Deficient Tumours with Inhibitors of Poly(ADP-ribose) Polymerase. *Nature* **2005**, *434*, 913−917.

(2) Curtin, N.; Szabo, C. Therapeutic Applications of PARP Inhibitors: Anticancer Therapy and Beyond. *Mol. Aspects Med.* **2013**, *24*, 1217−1256.

(3) De Rycker, M.; Price, C. M. Tankyrase Polymerization Is Controlled by Its Sterile Alpha Motif and Poly(ADP-ribose) Polymerase Domains. *Mol. Cell. Biol.* **2004**, *24*, 9802−9812.

(4) Riffell, J. L.; Lord, C. J.; Ashworth, A. Tankyrase-Targeted Therapeutics: Expanding Opportunities in the PARP Family. *Nat. Rev. Drug Discovery* **2012**, *11*, 923−936.

(5) Lehtiö, L.; Chi, N.-W.; Krauss, S. Tankyrases as Drug Targets. *FEBS J.* **2013**, *280*, 3576−3593.

(6) Lau, T.; Chan, E.; Callow, M.; Waaler, J.; Boggs, J.; Blake, R. A.; Magnuson, S.; Sambrone, A.; Schutten, M.; Firestein, R.; et al. A Novel Tankyrase Small-Molecule Inhibitor Suppresses APC Mutation-Driven Colorectal Tumor Growth. *Cancer Res.* **2013**, *73*, 3132−3144.

(7) Narwal, M.; Fallarero, A.; Vuorela, P.; Lehtiö, L. Homogeneous Screening Assay for Human Tankyrase. *J. Biomol. Screening* **2012**, *17*, 593−604.

(8) Kirby, C. A.; Cheung, A.; Fazal, A.; Shultz, M. D.; Stams, T. Structure of Human Tankyrase 1 in Complex with Small-Molecule Inhibitors PJ34 and XAV939. *Acta Crystallogr., Sect. F: Struct. Biol. Cryst. Commun.* **2012**, *68*, 115−118.

(9) Wahlberg, E.; Karlberg, T.; Kouznetsova, E.; Markova, N.; Macchiarulo, A.; Thorsell, A.-G.; Pol, E.; Frostell, A.; Ekblad, T.; Oncü, D.; et al. Family-Wide Chemical Profiling and Structural Analysis of PARP and Tankyrase Inhibitors. *Nat. Biotechnol.* **2012**, *30*, 283−288.

(10) Narwal, M.; Venkannagari, H.; Lehtiö, L. Structural Basis of Selective Inhibition of Human Tankyrases. *J. Med. Chem.* **2012**, *55*, 1360−1367.

(11) Menear, K. A.; Adcock, C.; Boulter, R.; Cockcroft, X.; Copsey, L.; Cranston, A.; Dillon, K. J.; Drzewiecki, J.; Garman, S.; Gomez, S.; et al. 4-[3-(4-Cyclopropanecarbonylpiperazine-1-carbonyl)-4-fluorobenzyl]-2*H*-phthalazin-1-one: A Novel Bioavailable Inhibitor of Poly(ADP-ribose) Polymerase-1. *J. Med. Chem.* **2008**, *51*, 6581−6591.

(12) Karlberg, T.; Markova, N.; Johansson, I.; Hammarström, M.; Schütz, P.; Weigelt, J.; Schüler, H. Structural Basis for the Interaction between Tankyrase-2 and a Potent Wnt-Signaling Inhibitor. *J. Med. Chem.* **2010**, *53*, 5352−5355.

(13) Huang, S.-M. A.; Mishina, Y. M.; Liu, S.; Cheung, A.; Stegmeier, F.; Michaud, G. A.; Charlat, O.; Wiellette, E.; Zhang, Y.; Wiessner, S.; et al. Tankyrase Inhibition Stabilizes Axin and Antagonizes Wnt Signalling. *Nature* **2009**, *461*, 614−620.

(14) Narwal, M.; Haikarainen, T.; Fallarero, A.; Vuorela, P.; Lehtiö, L. Screening and Structural Analysis of Flavones Inhibiting Tankyrases. *J. Med. Chem.* **2013**, *56*, 3507−3517.

(15) Jagtap, P. G.; Southan, G. J.; Baloglu, E.; Ram, S.; Mabley, J. G.; Marton, A.; Salzman, A.; Szabó, C. The Discovery and Synthesis of Novel Adenosine Substituted 2,3-Dihydro-1*H*-isoindol-1-ones: Potent Inhibitors of Poly(ADP-ribose) Polymerase-1 (PARP-1). *Bioorg. Med. Chem. Lett.* **2004**, *14*, 81−85.

(16) Banasik, M.; Komura, H.; Shimoyama, M.; Ueda, K. Specific Inhibitors of Poly(ADP-ribose) Synthetase and Mono(ADP-ribosyl)-transferase. *J. Biol. Chem.* **1992**, *267*, 1569−1575.

(17) Chiarugi, A.; Meli, E.; Calvani, M.; Picca, R.; Baronti, R.; Camaioni, E.; Costantino, G.; Marinozzi, M.; Pellegrini-Giampietro, D. E.; Pellicciari, R.; et al. Novel Isoquinolinone-Derived Inhibitors of Poly(ADP-ribose) Polymerase-1: Pharmacological Characterization and Neuroprotective Effects in an in Vitro Model of Cerebral Ischemia. *J. Pharmacol. Exp. Ther.* **2003**, *305*, 943−949.

(18) Thomas, H. D.; Calabrese, C. R.; Batey, M. A.; Canan, S.; Hostomsky, Z.; Kyle, S.; Maegley, K. A.; Newell, D. R.; Skalitzky, D.; Wang, L.-Z.; et al. Preclinical Selection of a Novel Poly(ADP-ribose) Polymerase Inhibitor for Clinical Trial. *Mol. Cancer Ther.* **2007**, *6*, 945−956.

(19) Jagtap, P.; Soriano, F. G.; Virag, L.; Liaudet, L.; Mabley, J.; Szabo, E.; Hasko, G.; Marton, A.; Lorigados, C. B.; Gallyas, F.; et al. Novel Phenanthridinone Inhibitors of Poly(adenosine ′5-diphosphate-ribose) Synthetase: Potent Cytoprotective and Antishock Agents. *Crit. Care Med.* **2002**, *30*, 1071−1082.

(20) Sinnberg, T.; Menzel, M.; Ewerth, D.; Sauer, B.; Schwarz, M.; Schaller, M.; Garbe, C.; Schittek, B. B-Catenin Signaling Increases during Melanoma Progression and Promotes Tumor Cell Survival and Chemoresistance. *PloS One* **2011**, *6*, e23429.

(21) Liu, X.; Mazanek, P.; Dam, V.; Wang, Q.; Zhao, H.; Guo, R.; Jagannathan, J.; Cnaan, A.; Maris, J. M.; Hogarty, M. D. Deregulated Wnt/beta-Catenin Program in High-Risk Neuroblastomas without MYCN Amplification. *Oncogene* **2008**, *27*, 1478−1488.

(22) Bell, C. E.; Eisenberg, D. Crystal Structure of Diphtheria Toxin Bound to Nicotinamide Adenine Dinucleotide. *Biochemistry* **1996**, *35*, 1137−1149.

(23) Haikarainen, T.; Venkannagari, H.; Narwal, M.; Obaji, E.; Lee, H.-W.; Nkizinkiko, Y.; Lehtiö, L. Structural Basis and Selectivity of Tankyrase Inhibition by a Wnt Signaling Inhibitor WIKI4. *PLoS One* **2013**, *8*, e65404.

(24) Voronkov, A.; Holsworth, D. D.; Waaler, J.; Wilson, S. R.; Ekblad, B.; Perdreau-Dahl, H.; Dinh, H.; Drewes, G.; Hopf, C.; Morth, J. P.; et al. Structural Basis and SAR for G007-LK, a Lead Stage 1,2,4-Triazole Based Specific Tankyrase 1/2 Inhibitor. *J. Med. Chem.* **2013**, *56*, 3012−3023.